THE ASTROPHYSICAL JOURNAL, 535:247–255, 2000 May 20

EVOLVING OPTICAL PROPERTIES OF ANNEALING SILICATE GRAINS: FROM AMORPHOUS CONDENSATE TO CRYSTALLINE MINERAL

SUSAN L. HALLENBECK
Astrochemistry Branch, Code 691, NASA Goddard Space Flight Center, Greenbelt, MD 20771; Susan.Hallenbeck@gsfc.nasa.gov
JOSEPH A. NUTH III
Astrochemistry Branch, Code 691, NASA Goddard Space Flight Center, Greenbelt, MD 20771; Joseph.Nuth@gsfc.nasa.gov
AND
ROBERT N. NELSON
Chemistry Department, Georgia Southern University, Statesboro, GA 30460; Robert_N_Nelson@GaSoU.edu
Received 1999 January 28; accepted 1999 August 17

ABSTRACT

Laboratory studies of the evolution of a magnesium silicate smoke from an amorphous condensate to a crystalline mineral by annealing in vacuum provide a foundation for the development of a silicate evolution index (SEI). The SEI can be used to predict the emergent IR spectrum of silicate dust in a circumstellar shell based on the time-temperature history of the silicate grains in the outflow. Optical constants for the magnesium silicate smoke samples compatible with those of Draine & Lee are derived over the range 0.001–1000 μm.

Subject headings: circumstellar matter — dust, extinction — ISM: molecules — methods: laboratory — molecular processes

1. INTRODUCTION

The availability of the large *IRAS* Low-Resolution Spectrometer (LRS) database, classified by spectral shape (Cheeseman et al. 1989) and emissivity classes, has spurred a steady increase in efforts to model the emergent spectra of stars shrouded in dust. Collison & Fix (1991) presented a generalized model of axisymmetric dust emission for use in distinguishing the geometry of dust shells, in particular the difference between "donut-like" and "disklike" grain distributions that might apply to protostellar sources or to late-type stars. Simpson (1991) derived the variation in the shapes of the 10 and 18 μm silicate features observed in a sample of 117 stars with optically thin dust shells. While the shape of the 18 μm feature remained relatively constant, in the peak position and width of the 10 μm silicate feature there was considerable variation, which was attributed to several potential factors: grain size, grain composition, and optical depth effects. Ivezic & Elitzur (1995) studied the infrared emission and dynamics of outflows from late-type stars and found considerable differences in the outflow characteristics of the shell depending upon the composition of the grains. These models not only differentiated oxygen-rich from carbon-rich outflows but also found significant differences between shells containing graphite versus carbonaceous grains or crystalline olivine versus "astronomical silicate." Hron, Aringer, & Kerschbaum (1997) have recently extended studies by Little-Marenin & Little (1990) to a larger sample of oxygen-rich semiregular (SR) and Mira variables. They found a large degree of variation in the width and peak position of the 10 μm silicate feature but no clear association of this variation with other stellar parameters. They found that the most reasonable explanation for the variation in the character of the 10 μm emission feature was "changing contributions from olivine and corundum possibly caused by an increasing amount of dust processing..." (Hron et al. 1997).

We recently completed a study of the spectral evolution of an amorphous magnesium silicate smoke annealed in vacuum at temperatures ranging from 1000 to 1200 K (Hallenbeck, Nuth, & Daukantas 1998). The IR spectra of the annealed smokes displayed characteristic bands diagnostic of the degree of thermal evolution of the samples. The initial condensate had a peak absorbency at 9.3 μm that quickly shifted to 9.7 μm after several hours of annealing at 1027 K. After only 10.5 hr of annealing the smoke developed dual maxima at 9.8 and 11.1 ± 0.2 μm: at low resolution this would certainly appear to be a broad asymmetric peak with a center at about 10.5 μm. The shape and overall peak position of the 20 μm feature evolved very little during this same time period. No significant changes were observed in the 10 μm region of the silicate spectrum during the next 37.5 hr of annealing: there appears to be a natural pause or "stall" in the spectral evolution of the sample, midway between the initially chaotic condensate and the more ordered glass. Thereafter, individual features sharpened as the sample became more ordered. The annealed smoke displayed the same evolutionary stages over the temperature range studied, but the rate of spectral change was highly temperature dependent.

Transmission electron microscopy (TEM) analysis of the initial smoke sample (Nuth, Hallenbeck, & Rietmeijer 1999) reveals a mixture of 20–30 nm diameter amorphous magnesium silicate grains that span a broad range of Mg/Si ratios peaking at compositions approximating the smectite ($Mg_6Si_8O_{22}$) and serpentine ($Mg_3Si_2O_7$) dehydroxylates. In addition, there are in the mixture large (200–400 nm diameter) polycrystalline tridymite grains, which are experimental artifacts of the vapor phase condensation process. Analysis of the annealed samples shows that these two populations of grains remain compositionally isolated during annealing and do not readily exchange material. All stall samples showed evidence for polycrystalline forsterite and tridymite with the random appearance of enstatite (Nuth et al. 1999). With increased residence in the stall, the short-range order gave way to long-range crystallographic order in the nanograins. Once thermal annealing took the

smoke out of the stall, long-range order improved on scales larger than individual nanograins and grain growth proceeded to a point where irregularly shaped single-crystal magnesium silicates could develop.

Examination of the spectra of the evolving magnesium silicate smokes and comparison to the observed spectra of dusty comets (Hanner et al. 1994) reveals remarkable agreement between the position and shape of the spectra of the natural particles and those of our synthetic analogs with one exception: natural particles contain little free silica (e.g., they have no peaks at $\sim$9.2 or 12.5 μm). Fortunately, it is relatively easy to quantitatively subtract the contribution of the pure silica component from the spectra of our annealed smokes to obtain the spectra of the magnesium silicate grains at any stage in the annealing process. In this paper we will present two series of spectra, the original IR spectra of the annealed laboratory samples and the "silica-free" magnesium silicate spectra, representing successive stages of evolution beginning with fresh condensates and proceeding through nearly crystalline forsterite and tridymite.

We have developed a silicate evolution index based on our measurements of the rate of change observed in our synthetic silicate smokes as a function of annealing temperature. This index is keyed to spectra representative of the stall stage of evolution and is calculable based on the time-temperature history of grains in a circumstellar outflow. This index and its application are discussed in §§ 2 and 3. In § 4, the silica-subtracted spectra have been converted into appropriate optical constants over the wavelength interval used by Draine & Lee (1984). These constants have been chosen so that the annealed magnesium silicate spectra are consistent with and blend smoothly into the spectrum of astronomical silicate derived by Draine & Lee (1984). Finally, we will stress the many caveats that need to be applied to these results and the fact that much more effort is needed to quantify various aspects of the silicate evolution index presented below.

2. SILICATE EVOLUTION INDEX

Hallenbeck et al. (1998), hereafter HND, demonstrated the temperature dependence of the spectral evolution of a magnesium silicate smoke, beginning with a highly amorphous condensate and ending with relatively ordered forsterite crystals. This laboratory investigation provides a database, which can be used to predict astronomical spectra based on the time-temperature profiles of silicate grains in circumstellar outflows. In order to quantify the degree of silicate evolution, it is necessary to account for the spectral stall (Fig. 1). The annealing times required to enter and exit the stall at a specific temperature are given by equations (1) and (2), respectively, where time (t) is in seconds and temperature (T) is in kelvins:

$$t_{\rm in} = 1.3 \times 10^{-55} \exp\,(140{,}870/T)\,, \quad (1)$$

$$t_{\rm out} = 1.7 \times 10^{-70} \exp\,(177{,}430/T)\,. \quad (2)$$

These equations can be recast to yield a measure of the annealing path traversed if a grain spends a known interval of time at a particular temperature. If we define $f_{\rm in}$ and $f_{\rm out}$ as the fraction of the annealing required to reach or exit the stall, respectively, then

$$f_{\rm in} = 7.77 \times 10^{54} t \exp\,(-140{,}870/T)\,, \quad (3)$$

$$f_{\rm out} = 5.88 \times 10^{69} t \exp\,(-177{,}430/T)\,. \quad (4)$$

Integration of these two equations for a given time-temperature path in a circumstellar outflow will yield a value of 1 when the condensate has been annealed sufficiently to have reached (eq. [3]) or to have begun to evolve from (eq. [4]) the spectral stall. Note that, whereas $f_{\rm in}$ becomes relatively meaningless after reaching 1, the stall spectrum, $f_{\rm out}$ does not, since it tracks the subsequent evolution of the silicate toward crystallinity. Note also that because $f_{\rm in}$ and $f_{\rm out}$ have different slopes the integrations must be done independently.

The silicate evolution index (SEI) tracks the cumulative degree of annealing using both equations (3) and (4) in the following fashion:

$$\mathrm{SEI} = A + B\,, \quad (5)$$

where

$$A = f_{\rm in},\ B = 0 \quad \text{for} \quad 0 \le f_{\rm in} \le 1,\ T < 1067\ \mathrm{K}\ ;$$

$$A = 1,\ B = f_{\rm out} \quad \text{for} \quad f_{\rm in} > 1,\ T < 1067\ \mathrm{K}\ ;$$

$$A = 1,\ B = f_{\rm out} \quad \text{for} \quad T \ge 1067\ \mathrm{K}\,.$$

Values of SEI less than 1 therefore indicate silicate

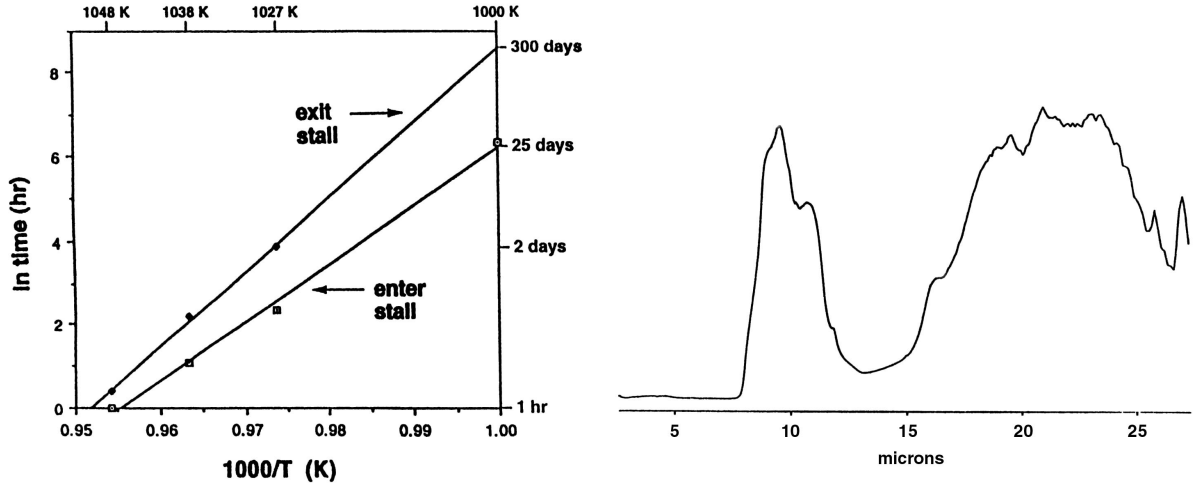

FIG. 1.—IR spectrum representative of the magnesium silicate stall and an Arrhenius plot of the time required for the smoke sample to enter and exit the stall phase of evolution.

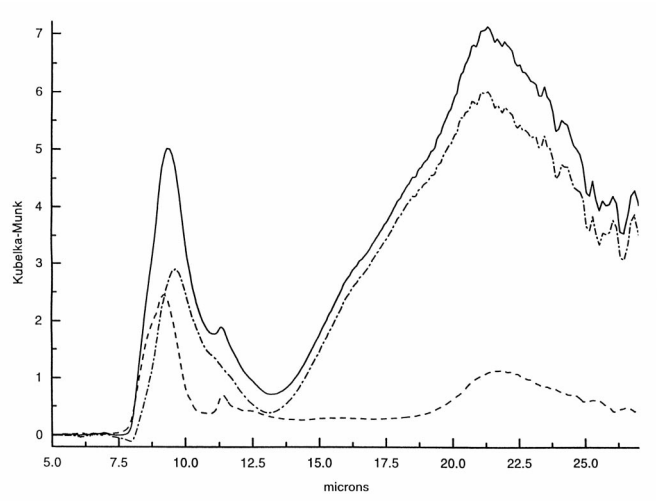

FIG. 2.—IR spectra of the initial magnesium silicate condensate containing free silica (*solid line*), a pure silica condensate (*dashed line*), and the calculated subtraction spectra representing a "pure" magnesium silicate condensate (*dot-dashed line*).

spectra that have not yet reached the stall. Values between 1 and 2 indicate that the stall has been reached but not exceeded, whereas for values greater than 2 the grain spectra are progressing from the stall toward crystallinity. Note that the value of SEI is discontinuous at $A = 1$; however, since all stall spectra are identical, this discontinuity will have no practical effect in the application of the SEI to astrophysical problems.

Careful inspection of equations (1) and (2) will reveal that these curves should intersect at some temperature, above which the spectral evolution of magnesium silicates proceeds without a stall. Equating t_{in} with t_{out} and solving for T yields a temperature of 1067 K at which no stall in the evolution of magnesium silicates occurs. Using either equation (1) or (2) shows that magnesium silicate condensates reach and pass through the stall spectrum at 1067 K in 281 s and then begin to evolve toward crystallinity. Therefore, as noted above, equation (5) is strictly valid only for temperatures less than 1067 K. For temperatures greater than 1067 K, f_{in} has no meaning. Because of the rapidity at which annealing occurs at $T \geq 1067$ K, the discontinuity in SEI at this temperature will have little practical effect in the choice of the optical properties used to calculate the grain spectrum, provided that A is set to 1 for consistency with lower temperature results.

3. APPLICATION OF THE SEI

The magnesium silicate smoke described in HND also contains a polycrystalline tridymite component responsible for substructure in the 10 and 20 μm features. In order to make the optical constants presented in this paper more universally applicable to oxygen-rich circumstellar regions, we have subtracted the spectrum of pure silica smoke from the spectra of the magnesium silicate sample containing free silica. For example, the IR spectra of the initial magnesium silicate condensate from HND and of a pure silica condensate produced under comparable experimental conditions are shown in Figure 2, along with the calculated silica-free magnesium silicate spectrum. Subtracting the pure silica component causes the maximum for the 10 μm magnesium silicate peak to shift from 9.3 to 9.7 μm, the value typically reported for amorphous astronomical silicates. The subtraction process also results in the elimination of the Si_2O_3 peak at 11.3 μm and in a slight reduction in the intensity of the 20 μm feature.

The spectra selected to represent the thermal evolution of a magnesium silicate grain from an amorphous material to a crystalline mineral are shown in Figure 3. We have included four prestall spectra, a stall spectrum, and four poststall spectra, along with their calculated SEI values ranging from 0.002 to 31.16. For SEI values greater than 100, we recommend that optical constants of appropriate crystalline phases, such as those of Koike, Shibai, & Tsuchiyama (1993), be used.

The spectra in Figure 3 were obtained by annealing the magnesium silicate smoke under conditions ranging from 1 hr at 1000 K (SEI = 0.002) to 48 hr at 1048 K (SEI = 31.16). Pure silica smoke annealed for these two sets of time and

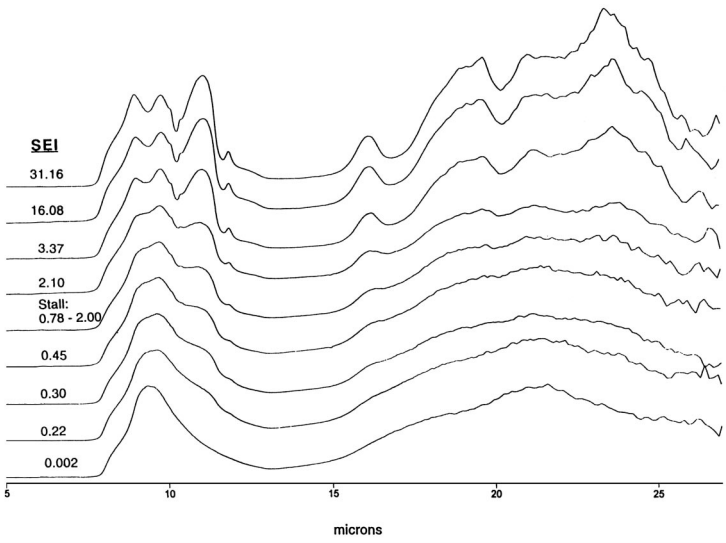

FIG. 3.—IR spectra of magnesium silicate smoke samples containing free silica annealed in vacuum and their silicate evolution index values (0.002–31.16).

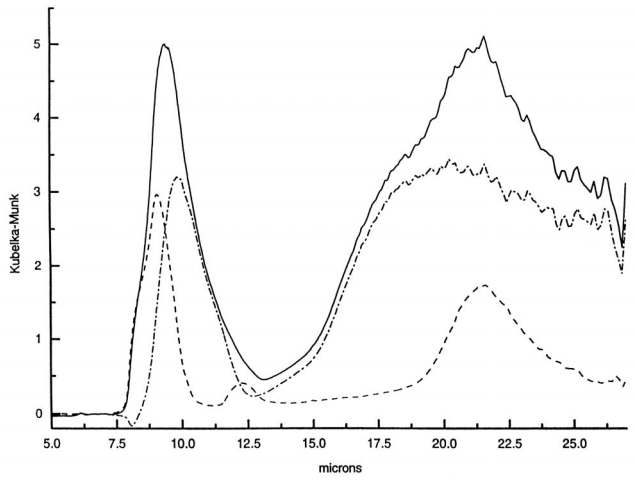

FIG. 4.—IR spectra of an annealed magnesium silicate sample with a SEI value of 0.002 (*solid line*), an annealed pure silica sample (*dashed line*), and the calculated silica-free magnesium silicate spectra (*dot-dashed line*).

temperature display identical IR spectra: a peak at 9.08 μm, which can be deconvolved into bands centered at 8.35 and 9.00 μm, and peaks at 12.22 and 21.59 μm (Fig. 4). Although the same annealed silica spectrum was used for all the subtractions, the integrated intensity of the silica spectrum ranged from 20% to 26% of the integrated intensity of the annealed magnesium silicate samples. The exact percentage employed in each subtraction was determined by the minimum amount of silica necessary to account for the 8.35 and 12.22 μm substructure in the 10 μm feature. This range in silica abundance is attributed to compositional variations between the individual magnesium silicate aliquots extracted from the bulk sample.

An example of silica subtraction from an annealed magnesium silicate smoke (SEI = 0.002) is shown in Figure 4, and the complete set of calculated, silica-free magnesium silicate spectra for SEIs 0.002–31.16 is presented in Figure 5. Subtraction of the pure silica component from the stall spectrum changes the ratio of the 9.8 and 11 μm peaks from 1.0:0.7 to 1.0:0.9, which is much closer to the ratio observed for olivine-rich comets (Hanner et al. 1994). For the highly evolved samples, the silica-free spectra resemble the spectra of crystalline forsterite with a small contribution due to enstatite (Koike et al. 1993), in complete agreement with the TEM analysis. Although subtraction of the pure silica component had little effect on the 20 μm feature of the initial condensate, in the annealed samples the prestall silica-free spectra display flatter 20 μm features that peak at shorter wavelengths, while the stall and poststall spectra have more forsteritic 20 μm signatures.

4. DERIVATION OF OPTICAL CONSTANTS

No optical constants were measured during the course of the experiments outlined in HND because of the small size of the samples ($\sim$5 mg) used in the individual annealing runs. After obtaining the diffuse reflectance spectrum of each sample, the annealed smokes were sent to a colleague for TEM analysis so that the mid-IR spectra of the samples might eventually be used to constrain both the composition and mineralogical texture of grains in astrophysical sources. However, it is still possible to use the method outlined by Draine & Lee (1984) to derive a self-consistent set of optical constants for our samples. In our application we will assume that the magnesium silicate smoke samples have nearly the same optical constants as astronomical silicate over all wavelengths except over the range from 5 to 27 μm and that each annealed silicate spectrum connects smoothly with that of astronomical silicate at these wavelengths.

Although the assumptions outlined above are essential if we wish to derive a complete set of optical constants over the wavelength range from 100 nm to 1000 μm, they are also not that unreasonable as a first approximation. Draine & Lee (1984) derived the optical constants for astronomical silicate to represent the amorphous oxide component of the interstellar grain population. Amorphous magnesium and iron silicates should dominate this population based on cosmic abundance considerations. The mid-infrared spectra of iron and magnesium silicates are quite similar in general, even though magnesium silicates anneal much more rapidly than do iron silicates (HND). Given the fact that amorphous magnesium and iron silicates show no strong spectral features at wavelengths other than in the mid-infrared and

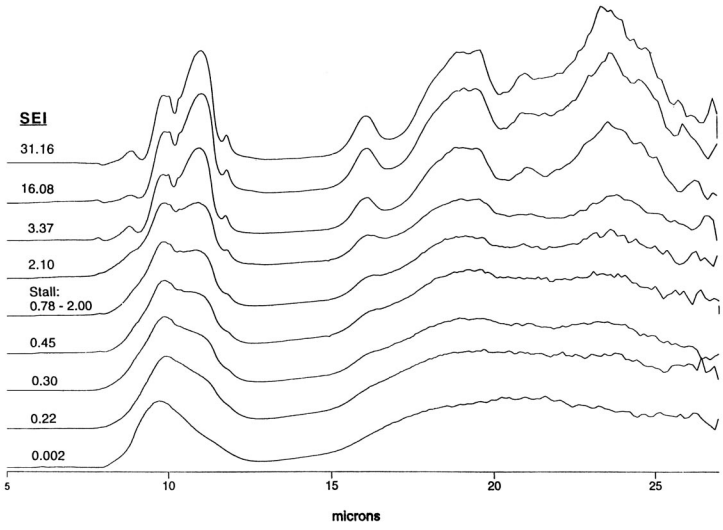

FIG. 5.—Calculated silica-free IR spectra for annealed magnesium silicate samples spanning a SEI range of 0.002–31.16

that the Draine & Lee constants are already used to represent the spectral properties of the grain population dominated by these silicates, the Draine & Lee astronomical silicate spectrum appears to be a good first approximation to the spectra of the grains in our sample at wavelengths that we could not measure in our study.

The 5–25 μm spectrum of astronomical silicate has been replaced by the mid-infrared spectra of the annealed samples measured in our study by smoothly scaling the measured spectra to match that of Draine & Lee (1984) at these wavelengths. This could potentially overestimate the contribution of magnesium silicate to the Draine & Lee constants by overlooking the contribution of amorphous iron silicate in this region. However, if iron is present as metal in a circumstellar condensate as predicted by thermodynamic calculations (Ebel 1999; Grossman 1972), then there is no iron silicate condensate in this grain population. Even if iron silicates condense separately in such outflows (Rietmeijer et al. 1999), because the iron silicate spectrum should remain constant over the temperature range of interest ($T < 1100$ K) in this paper, our approximation maximizes the contribution of the changing component of the grain population. Because there will likely be additional unchanging spectral components in this condensed mixture as well, most models will need to incorporate an appropriately scaled, unchanging graybody into the grain population. We suggest that an appropriate, near graybody would be the difference spectrum between our original amorphous magnesium silicate smokes and the spectrum of astronomical silicate; the optical constants for this hypothetical grain component have also been calculated.

There is no question that direct measurement of the optical constants of our samples would have been preferable to calculations based on the approximations outlined above; unfortunately, this was not possible. Given the utility of a set of optical constants versus a collection of spectral plots over a limited wavelength range (such as Fig. 5) in the construction of models of stellar extinction or emission due to grains, we decided that derivation of a self-consistent set of optical constants could prove to be worthwhile. However, in spite of our best efforts to calculate these constants based on reasonable approximations and in a manner consistent with our original laboratory measurements, we caution the reader that these constants should be regarded with some degree of skepticism. At best, they are only a first approximation to reality, especially with regard to the non–magnesium-silicate grain components. Considerable laboratory work remains to be carried out to measure the optical properties of these grain components.

Given the assumptions outlined above together with the methods presented and constants tabulated in the work of Draine & Lee (1984), it is a relatively straightforward task to convert our measurements into a set of self-consistent optical constants over the wavelength range of interest. The complete set of optical constants from 100 nm to 1000 μm calculated for the magnesium silicate spectra minus the silica component (Figs. 2 and 5) and for the pure silica spectra (Figs. 2 and 4) are presented in Tables 1, 2, and 3.[1] Table 4 is an abbreviated version of Tables 1–3 covering the mid-IR region for prestall, stall, and poststall grains.

We note here one obvious shortcoming of this method: namely, neither the long-wavelength nor the short-wavelength properties of the grains are allowed to change as the silicate transforms from a highly amorphous condensate into what might well be a completely crystalline grain. This will be most important in the far-infrared, where the falloff varies from somewhat less than λ^{-1} for highly amorphous materials (e.g., Harvey et al. 1991) to λ^{-2} for crystalline grains (Koike et al. 1993). For SEI < 1 (prestall) the compositional heterogeneities within individual amorphous grains are becoming homogenized and individual subgrain boundaries begin to develop, whereas for $1 \leq \mathrm{SEI} \leq 2$ individual grains exhibit polycrystalline textures consisting of many smaller subcrystalline units (F. J. M. Rietmeijer 1998, private communication). Neither of these textures would be expected to exhibit λ^{-2} behavior as both would be amorphous on size scales of a few microns to a few hundred microns, the wavelength of the radiation in question.

For SEI > 2, the individual subgrain boundaries begin to anneal away and crystalline minerals eventually form. For models in which the long-wavelength behavior of the grains becomes important, some smooth transition between the λ^{-1} behavior of amorphous materials and the λ^{-2} behavior of crystalline solids is required. We would suggest that for SEI > 102 silicate condensates should be considered to be completely crystalline and the optical constants of Koike et

[1] Tables 1, 2, and 3 appear in their entirety in the electronic edition of the Astrophysical Journal.

TABLE 1

OPTICAL CONSTANTS

Wavelength (μm)	Magnesium Silicate (Unannealed)		Prestall 1 (SEI = 0.002)		Prestall 2 (SEI = 0.223)		Prestall 3 (SEI = 0.298)		Prestall 4 (SEI = 0.447)	
	Re	Im	Re	Im	Re	Im	Re	Im	Re	Im
0.001	−0.000692	0	−0.00069	0	−0.000693	0	−0.00069	0	−0.000677	0
0.00101	−0.000696	0	−0.000695	0	−0.000695	0	−0.000694	0	−0.000693	0
0.00102	−0.000699	0	−0.000699	0	−0.000697	0	−0.000698	0	−0.000682	0
0.00104	−0.000703	0	−0.000705	0	−0.000701	0	−0.000704	0	−0.000712	0
0.00105	−0.000712	0	−0.000714	0	−0.000711	0	−0.000714	0	−0.00072	0
0.00106	−0.000726	0	−0.000728	0	−0.000727	0	−0.000728	0	−0.000731	0
0.00107	−0.000745	0	−0.000745	0	−0.000747	0	−0.000746	0	−0.000744	0
0.00108	−0.000765	0	−0.000764	0	−0.000768	0	−0.000765	0	−0.000754	0
0.0011	−0.000785	0	−0.000783	0	−0.000786	0	−0.000783	0	−0.000782	0
0.00111	−0.000801	0	−0.0008	0	−0.000801	0	−0.0008	0	−0.000794	0

NOTE.—Table 1 is published in its entirety in the electronic edition of The Astrophysical Journal. A portion is shown here for guidance regarding its form and content.

TABLE 2

OPTICAL CONSTANTS

WAVELENGTH (μm)	STALL (SEI = 1.000)		POSTSTALL 1 (SEI = 2.104)		POSTSTALL 2 (SEI = 3.336)		POSTSTALL 3 (SEI = 16.078)		POSTSTALL 4 (SEI = 31.156)	
	Re	Im	Re	Im	Re	Im	Re	Im	Re	Im
0.001	−0.000694	0	−0.000697	0	−0.000699	0	−0.000702	0	−0.000705	0
0.00101	−0.000695	0	−0.000697	0	−0.000694	0	−0.000697	0	−0.000699	0
0.00102	−0.000696	0	−0.000695	0	−0.000689	0	−0.000691	0	−0.000691	0
0.00104	−0.0007	0	−0.000697	0	−0.000691	0	−0.00069	0	−0.000688	0
0.00105	−0.00071	0	−0.000707	0	−0.000704	0	−0.000701	0	−0.000698	0
0.00106	−0.000726	0	−0.000724	0	−0.000726	0	−0.000722	0	−0.00072	0
0.00107	−0.000747	0	−0.000747	0	−0.000753	0	−0.000751	0	−0.00075	0
0.00108	−0.000769	0	−0.000771	0	−0.000778	0	−0.000778	0	−0.000779	0
0.0011	−0.000788	0	−0.000791	0	−0.000795	0	−0.000798	0	−0.0008	0
0.00111	−0.000802	0	−0.000805	0	−0.000804	0	−0.000808	0	−0.000811	0

NOTE.—Table 2 is published in its entirety in the electronic edition of The Astrophysical Journal. A portion is shown here for guidance regarding its form and content.

al. (1993) should be used to calculate the optical properties of the grains. For $2 < \mathrm{SEI} < 102$ we suggest that a smooth transition between the optical constants of Drain & Lee (1984) and those of Koike can easily be achieved by a linear combination of grain spectra calculated from the two data sets. In this method the percentage of grains calculated from the constants of Draine & Lee is equal to $(102 - \mathrm{SEI})/100$ and that of grains calculated using the constants of Koike equal $(\mathrm{SEI} - 2)/100$. Note that we have simply assumed that for $\mathrm{SEI} > 102$ the grains will behave as crystalline materials. We have not measured this transition in the laboratory partially because of the difficulty in judging at just what point an annealing amorphous solid does indeed become crystalline and partially because this transition is expected to be highly sensitive to the experimental method used in the measurement. However, for the purposes of virtually all astrophysical applications, grains annealed to $\mathrm{SEI} > 102$ will behave as crystalline materials.

As noted above, the astronomical silicate of Draine & Lee (1984) includes all noncarbonaceous grain materials, not just magnesium silicates. For this reason, we have included optical constants for a nonsilicate oxide component to the dust that might be found in oxygen-rich circumstellar shells. This component is derived by subtracting the spectrum of unannealed magnesium silicate smoke from the astronomical silicate of Draine & Lee (Fig. 6). Since we know nothing about the annealing behavior of this grain component, we will assume that its spectrum does not change at all in most circumstellar outflows. Although this might be a reasonable first approximation, it is clear that much more work is needed both to identify likely oxide grain components and to measure the spectral changes induced in these materials during annealing.

5. CAVEATS IN USING THE SEI AND ASSOCIATED SPECTRA

All of the spectra of annealed silicates in Figure 3 were derived from a single bulk sample of highly amorphous magnesium silicate smoke. HND have noted that both the annealing rate and sample spectrum at any given annealing time and temperature vary slightly if a sample of different composition or starting texture is used in the experiments. The magnitude of this compositional and textural dependence has not yet been determined. Several samples of mag-

TABLE 3

OPTICAL CONSTANTS

WAVELENGTH (μm)	DRAINE & LEE		MAGNESIUM SILICATE (UNANNEALED)		DRAINE & LEE MINUS MAGNESIUM SILICATE		ANNEALED SiO_x		UNANNEALED SiO_x	
	Re	Im	Re	Im	Re	Im	Re	Im	Re	Im
0.001	−0.000691	0	−0.000692	0	−0.000691	0	−0.0007	0	−0.0007	0
0.00101	−0.000695	0	−0.000696	0	−0.000695	0	−0.0007	0	−0.0007	0
0.00102	−0.000699	0	−0.000699	0	−0.000698	0	−0.0007	0	−0.0007	0
0.00104	−0.000705	0	−0.000703	0	−0.000704	0	−0.0007	0	−0.0007	0
0.00105	−0.000714	0	−0.000712	0	−0.000714	0	−0.0007	0	−0.0007	0
0.00106	−0.000727	0	−0.000726	0	−0.000728	0	−0.0007	0	−0.0007	0
0.00107	−0.000745	0	−0.000745	0	−0.000746	0	−0.0007	0	−0.0007	0
0.00108	−0.000764	0	−0.000765	0	−0.000765	0	−0.0008	0	−0.0008	0
0.0011	−0.000783	0	−0.000785	0	−0.000783	0	−0.0008	0	−0.0008	0
0.00111	−0.0008	0	−0.000801	0	−0.0008	0	−0.0008	0	−0.0008	0

NOTE.—Table 3 is published in its entirety in the electronic edition of The Astrophysical Journal. A portion is shown here for guidance regarding its form and content.

TABLE 4

OPTICAL CONSTANTS

	MAGNESIUM SILICATE (UNANNEALED)		PRESTALL 1 (SEI = 0.002)		PRESTALL 2 (SEI = 0.223)		PRESTALL 3 (SEI = 0.298)		PRESTALL 4 (SEI = 0.447)		STALL (SEI = 1.000)		POSTSTALL 1 (SEI = 2.104)		POSTSTALL 2 (SEI = 3.336)		POSTSTALL 3 (SEI = 16.078)		POSTSSTALL 4 (SEI = 31.156)	
WAVELENGTH	Re	Im	Re	Im	Re	Im	Re	Im	Re	Im	Re	Im	Re	Im	Re	Im	Re	Im	Re	Im
5.0	1.437	0.187	1.463	0.154	1.431	0.156	1.419	0.164	1.452	0.134	1.438	0.139	1.467	0.089	1.467	0.139	1.489	0.086	1.454	0.160
5.5	1.350	0.211	1.354	0.192	1.313	0.193	1.309	0.203	1.310	0.178	1.313	0.180	1.300	0.131	1.349	0.181	1.320	0.131	1.348	0.193
6.0	1.230	0.231	1.229	0.259	1.181	0.245	1.176	0.263	1.169	0.243	1.173	0.247	1.128	0.200	1.224	0.244	1.173	0.206	1.233	0.243
6.5	1.083	0.307	1.103	0.293	1.037	0.291	1.035	0.290	1.031	0.283	1.031	0.290	0.964	0.274	1.102	0.295	1.038	0.279	1.110	0.291
7.0	0.938	0.343	0.933	0.330	0.853	0.331	0.833	0.331	0.852	0.332	0.846	0.331	0.773	0.331	0.954	0.330	0.890	0.335	0.965	0.334
7.5	0.696	0.317	0.679	0.356	0.585	0.369	0.539	0.377	0.587	0.391	0.578	0.387	0.478	0.392	0.735	0.367	0.699	0.389	0.776	0.351
8.0	0.159	0.413	0.206	0.480	0.147	0.509	0.068	0.581	0.219	0.477	0.170	0.498	0.048	0.646	0.446	0.404	0.461	0.377	0.477	0.322
8.5	−0.423	1.273	−0.414	1.114	−0.428	1.008	−0.494	1.190	−0.420	0.951	−0.417	1.021	−0.384	1.228	−0.005	0.776	0.015	0.547	−0.003	0.623
9.0	−0.404	2.678	−0.657	2.696	−0.864	2.148	−0.811	2.420	−0.893	2.077	−0.818	2.077	−0.690	1.934	−0.459	0.932	−0.588	0.721	−0.427	0.867
9.5	0.515	3.414	0.209	3.886	−0.543	3.724	−0.384	3.895	−0.728	3.668	−0.609	3.617	−0.708	3.442	−1.029	2.696	−1.463	2.214	−1.256	2.102
10.0	1.514	2.886	1.535	3.738	0.673	4.325	0.854	4.355	0.591	4.280	0.523	4.316	0.249	4.371	−0.408	3.759	−1.056	4.007	−0.941	3.842
10.5	1.890	2.262	2.386	2.960	1.841	3.840	1.961	3.886	1.788	3.904	1.625	4.021	1.351	4.332	0.608	4.562	−0.067	4.760	−0.056	4.740
11.0	1.917	1.989	2.711	2.282	2.607	3.318	2.774	3.518	2.660	3.671	2.623	3.962	2.539	4.497	2.277	5.345	1.791	6.185	1.931	6.459
11.5	1.857	1.724	2.691	1.680	2.928	2.223	3.181	2.194	3.408	2.173	3.230	2.240	3.385	2.543	3.565	2.470	3.522	2.938	3.852	2.765
12.0	1.722	1.445	2.462	1.229	2.747	1.502	2.970	1.425	2.980	1.409	2.989	1.392	3.216	1.563	3.285	1.229	3.444	1.495	3.719	1.211
12.5	1.463	1.285	2.094	1.109	2.271	1.325	2.456	1.289	2.279	1.311	2.400	1.311	2.612	1.466	2.512	1.166	2.606	1.363	2.770	1.068
13.0	1.052	1.246	1.675	1.170	1.764	1.386	1.958	1.350	1.871	1.403	1.901	1.388	2.115	1.490	1.950	1.217	1.982	1.308	2.095	1.027
13.5	0.642	1.419	1.371	1.314	1.413	1.542	1.625	1.487	1.421	1.546	1.577	1.509	1.786	1.592	1.568	1.300	1.529	1.397	1.613	1.106
14.0	0.212	1.754	1.081	1.476	1.089	1.707	1.320	1.627	1.297	1.683	1.276	1.633	1.486	1.700	1.220	1.400	1.102	1.493	1.164	1.198
14.5	−0.091	2.203	0.833	1.658	0.804	1.883	1.048	1.775	0.968	1.832	0.995	1.759	1.204	1.801	0.867	1.504	0.695	1.630	0.738	1.316
15.0	−0.298	2.690	0.564	1.916	0.481	2.168	0.726	2.011	0.653	2.061	0.644	1.975	0.842	1.992	0.413	1.714	0.174	1.880	0.185	1.538
15.5	−0.386	3.208	0.340	2.333	0.225	2.687	0.469	2.524	0.139	2.610	0.366	2.493	0.579	2.558	0.121	2.464	−0.151	2.708	−0.164	2.350
16.0	−0.362	3.686	0.203	2.851	0.097	3.322	0.354	3.145	0.340	3.315	0.252	3.199	0.538	3.341	0.128	3.401	−0.092	3.886	−0.120	3.570
16.5	−0.300	4.042	0.212	3.342	0.127	3.771	0.386	3.470	0.135	3.617	0.263	3.393	0.590	3.258	0.147	2.887	−0.037	3.091	−0.106	2.636
17.0	−0.239	4.455	0.299	3.770	0.222	4.253	0.454	3.869	0.137	4.009	0.260	3.727	0.568	3.512	−0.037	3.086	−0.280	3.152	−0.436	2.626
17.5	−0.144	4.893	0.478	4.147	0.403	4.711	0.574	4.363	0.167	4.579	0.275	4.346	0.507	4.138	−0.336	4.051	−0.740	4.295	−1.028	3.865
18.0	0.012	5.325	0.716	4.434	0.674	5.117	0.794	4.774	0.343	5.225	0.437	5.011	0.598	4.885	−0.364	5.222	−0.896	5.776	−1.296	5.507
18.5	0.225	5.683	0.983	4.591	1.048	5.413	1.157	5.123	0.786	5.603	0.862	5.424	1.013	5.324	0.200	5.970	−0.289	6.758	−0.712	6.653
19.0	0.422	6.009	1.206	4.780	1.399	5.554	1.521	5.261	1.143	5.843	1.327	5.628	1.510	5.536	0.931	6.275	0.584	7.258	0.199	7.228
19.5	0.666	6.453	1.439	4.940	1.761	5.705	1.909	5.351	1.799	5.926	1.797	5.632	2.038	5.566	1.671	6.202	1.506	7.258	1.185	7.442
20.0	0.968	6.921	1.661	5.195	2.044	5.633	2.200	5.169	1.930	5.569	2.093	5.240	2.364	4.902	2.038	4.840	1.975	5.477	1.687	5.253
20.5	1.462	7.325	1.944	5.275	2.321	5.686	2.443	5.122	2.216	5.612	2.288	5.295	2.542	4.909	2.113	5.039	2.084	5.855	1.799	5.790
21.0	2.095	7.631	2.257	5.305	2.582	5.699	2.625	5.136	2.684	5.691	2.408	5.350	2.604	4.934	2.013	5.302	1.991	6.199	1.689	6.094
21.5	2.704	7.493	2.539	5.259	2.791	5.683	2.743	5.082	3.037	5.598	2.467	5.350	2.576	4.881	1.857	5.352	1.845	6.210	1.515	6.241
22.0	3.226	7.286	2.780	5.079	2.974	5.673	2.859	5.254	3.192	5.680	2.532	5.526	2.536	5.015	1.774	5.749	1.794	6.688	1.448	6.731
22.5	3.618	7.179	2.954	5.083	3.142	5.655	3.002	5.399	2.840	5.822	2.657	5.801	2.566	5.280	1.871	6.533	1.955	7.547	1.636	7.582
23.0	3.999	7.116	3.100	5.094	3.345	5.758	3.211	5.533	2.835	6.037	2.895	6.013	2.722	5.718	2.231	7.325	2.435	8.591	2.213	9.152
23.5	4.370	6.800	3.212	5.013	3.579	5.907	3.485	5.550	3.431	6.089	3.258	6.170	3.053	6.140	2.930	7.739	3.330	9.062	3.286	9.749
24.0	4.671	6.780	3.285	4.847	3.786	5.651	3.746	5.365	3.931	5.857	3.628	5.927	3.447	6.100	3.730	7.367	4.352	8.341	4.490	8.542
24.5	4.866	6.470	3.335	4.798	3.932	5.445	3.936	5.080	3.855	5.643	3.915	5.740	3.793	5.607	4.418	6.962	5.250	8.219	5.482	8.236
25.0	5.001	5.904	3.380	4.896	4.052	5.252	4.049	4.877	4.216	5.313	4.130	5.636	4.058	5.289	4.934	5.838	5.962	6.569	6.165	6.434

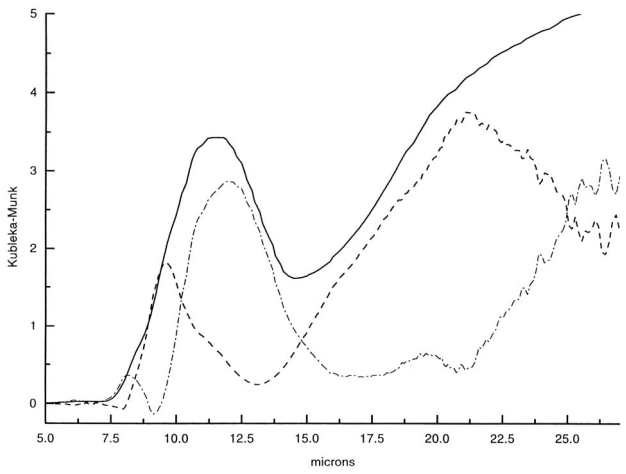

FIG. 6.—IR spectrum of astronomical silicate (Draine & Lee 1984) (*solid line*), the IR spectrum of unannealed silica-free magnesium silicate smoke (*dashed line*), and the IR spectrum of other oxide grains (*dot-dashed line*) that results from subtraction of the unannealed magnesium silicate spectrum from that of astronomical silicate.

nesium silicate starting materials have been examined and all exhibit a spectral stall. However, both the annealing time required at a given temperature to enter or exit the stall and the exact shape of the stall spectrum, e.g., the ratio of the 9.7 to 11 μm peak heights, differ slightly from the sample profiled in HND. A considerable amount of laboratory effort will be required to quantify the specific dependence of the stall spectrum and the rate of annealing on composition. Although the exact details of this evolution will become clearer as more data is obtained, we do not expect that our overall understanding of the spectral evolution of amorphous silicate smokes will change drastically.

The SEI is extremely sensitive to the highest temperatures experienced by the grains. These high temperatures occur at the time of grain formation—a very poorly understood phenomenon. If grains form at temperatures in excess of ~ 1100 K, they will quickly ($t < 10$ minutes) become crystalline. Grains formed at temperatures less than ~ 1000 K will almost never be annealed sufficiently in a typical circumstellar outflow to reach the stall. In either case, careful analysis of the emergent infrared spectrum of silicate dust in the circumstellar shell could be used to constrain the temperatures at which grain formation occurred.

In the case of optically thick dust envelopes, where interferometric methods are not possible, this might prove to be the only means of obtaining a measure of the grain formation radius. In optically thin shells, it may be possible to use interferometry to obtain a measure of the inner radius of the dust shell and thereby derive an independent measure of the dust formation temperature.

6. DISCUSSION

This paper is a first attempt to account for changing silicate optical properties as freshly condensed grains anneal in a circumstellar outflow or protostellar nebula. Although the details of the representative spectra and rate constants may change to some degree as future laboratory work allows us to refine the compositional or textural dependencies of these factors, we feel that this first attempt is a significant improvement over the current practice of using astronomical silicate to represent all stages of silicate grain evolution. Astronomical silicate is much more appropriately used as the average of the optical properties of grains from all oxygen-rich outflows rather than as representing grains in each outflow regardless of its temperature profile.

Again we note the extremely sharp dependence of the annealing rate of amorphous magnesium silicate grains on temperature. Because grain temperatures in most oxygen-rich outflows range from 300 to 600 K (Hron et al. 1997), most silicate grains will exhibit optical properties considerably more primitive than the stall spectrum; e.g., SEI < 1. In almost all such cases we expect that the detailed optical properties and annealing rates will vary little from those in this work because of compositional or textural factors since the differences in the initial stages of annealing are much less pronounced than they become at or beyond the stall stage.

Similarly, in high-temperature outflows the initially amorphous silicate condensates anneal quite rapidly to form crystalline grains. Under these circumstances we also expect little difference between our current results and more detailed analyses based on compositional or textural dependencies since annealing will occur so rapidly in these high-temperature flows that changes of a factor of 2, or even 10, in the annealing rate will be insignificant: e.g., if the SEI predicts the crystallization of forsterite in 30 s and it actually occurs in 3 s (or 5 minutes), the emergent spectrum of the source will not change.

For grain condensation temperatures on the order of $\sim 1030 \pm 30$ K, the exact rate of annealing may become extremely important since changes between factors of 2 and 10 in this range could mean the difference between prestall grains and crystalline forsterite emerging from the outflow. Unfortunately, since we do not know a priori the composition or texture of the grains that will condense in a given circumstellar outflow and we are still a long way from being able to model the nucleation and grain growth processes in such systems, more accurate laboratory data may not yet be needed. In fact, it may be possible to use a combination of modeling and observation to constrain the rate of annealing in actual circumstellar outflows. These models and observations would then serve as the basis for additional experimental studies that would use these constraints to identify the compositions and textures of the grains formed in such outflows.

7. SUMMARY

Using the experimental work presented in HND, we have developed a silicate evolution index (SEI) to describe the annealing of freshly condensed circumstellar or protostellar silicates. We have used the spectra of HND and the methods of Draine & Lee (1984) to derive a set of optical constants for silicate spectra representing different evolutionary stages. We suggest that these optical constants can be used together with the optical constants for astronomical silicate minus magnesium silicate (e.g., other oxides) to construct models of the infrared emission from circumstellar outflows and hot protostellar disks. Such models should represent a considerable improvement over the current state of the art, in which grain evolution is not considered.

We have noted several important caveats that should be kept in mind when using both the SEI and the optical constants provided in Tables 1, 2, and 3. First, the exact shape

of the infrared spectrum and the specific rate of annealing at any given temperature are dependent on the exact composition and mineralogical texture of the condensate. Although these variables should not effect condensates formed at either very high temperatures (fast conversion to crystallinity) or low temperatures (grains remain at a prestall evolutionary stage), for temperatures of $\sim 1030 \pm 30$ K more accurate laboratory data will be required to predict grain properties. Alternatively, observed grain properties could be used to constrain grain models, and laboratory data could then be used to determine the composition and mineralogical texture of the condensates.

An additional caveat is that the optical constants in Tables 1, 2, and 3 were derived, not measured, based on the spectra of HND and the spectrum calculated from the optical constants of astronomical silicate. In addition, the far-IR spectra of the annealed silicate samples were not obtained during our laboratory studies. For highly evolved samples (SEI $\gg$ 2) this omission could lead to considerable error in the optical constants of more crystalline materials. Alternatively, we have suggested an interpolation method using the spectra derived from constants for astronomical silicate (Draine & Lee 1984), crystalline forsterite (Koike et al. 1993), and a weighting factor based on the SEI that could serve as a reasonably good first approximation for the far-IR optical constants if such accuracy is required. Much more experimental, observational, and theoretical work will be required before grain formation and annealing in astrophysical environments are fully predictable phenomena.

This work is supported by NASA's Cosmochemistry Research Program. We thank Frans J. M. Rietmeijer of the Institute of Meteoritics at the University of New Mexico for helpful discussions and for assistance with the TEM analyses. S. L. H. is a NAS/NRC Resident Research Associate at GSFC.

REFERENCES

Cheeseman, P., Stutz, J., Self, M., Taylor, W., Goebel, J., Volk, K., & Walker, H. 1989, Automatic Classification of Spectra from the *Infrared Astronomical Satellite* (*IRAS*) (NASA RP-1217)
Collison, A. J., & Fix, J. D. 1991, ApJ, 368, 545
Draine, B. T., & Lee, H. K. 1984, ApJ, 285, 89
Ebel, D. 1999, J. Geophys. Res. (Space Phys.), in press
Grossman, L. 1972, Geochim. Cosmochim. Acta, 36, 597
Hallenbeck, S. L., Nuth, J. A., & Daukantas, P. L. 1998, Icarus, 131, 198 (HND)
Hanner, M. S., Hackwell, J. A., Russell, R. W., & Lynch, D. K. 1994, Icarus, 112, 490
Harvey, P. M., Lester, D. F., Brock, D., & Joy, M. 1991, ApJ, 368, 558
Hron, J., Aringer, B., & Kerschbaum, F. 1997, A&A, 322, 280
Ivezic, Z., & Elitzur, M. 1995, ApJ, 445, 415
Koike, C., Shibai, H., & Tuchiyama, A. 1993, MNRAS, 264, 654
Little-Marenin, I. R., & Little, S. J. 1990, AJ, 99, 1173
Nuth, J. A., Hallenbeck, S. L., & Rietmeijer, F. J. M. 1999, in Laboratory Astrophysics and Space Research, ed. P. Ehrenfreund & H. Kochan (Dordrecht: Kluwer), 143
Rietmeijer, F. J. M., et al. 1999, ApJ, 527, 395
Simpson, J. P. 1991, ApJ, 368, 570